Electrical behaviour of mono-Si based microhotplate heater

M. Mihailović, J.F. Creemer, P.M.Sarro

***Abstract*— This paper focuses on the electrical behaviour of monocrystalline silicon heater at different temperatures. The electrical resistivity of monocrystalline silicon rises with increasing temperature, starting from room temperature. After reaching the so-called intrinsic temperature of silicon, the resistivity drops significantly. Our heater, fabricated in a CMOS compatible process and aiming at temperatures up to 800 °C, is made of doped epitaxial mono-Si layer. Contact lines are made of titanium silicide. Four-point probe measurements of the heater resistance confirm the theoretical prediction and indicate that reached temperatures are above 600 °C. Comparison of the devices with the different active layers follow the prediction of shifting the intrinsic temperature to lower ranges for less doped silicon layers.**

***Index Terms*— hotplate, microheater, monocrystalline silicon, titanium silicide**

I. Introduction

MICROHEATERS are employed inside microsystems in a wide spectrum of applications [1-4]. They can increase the local temperature on the chip, while the rest of the chip remains at ambient temperature. Depending on the application, the achieved increases of temperature can vary from millilkelvins [5] to above 1000 K [6]. Sensing of the heater temperature is usually provided by monitoring the electrical resistance of the heater, which is temperature dependent.

Microheaters for high temperatures (reaching above 400 °C) have mainly chemical applications (microcalorimeters, gas sensors, microreactors). The most widespread devices use polycrystalline thin films as the heating elements (e.g. Pt, or poly-Si). However, these heaters express certain problems because of the polycrystalline structure and therefore cannot be employed successfully at very high temperatures [7]. Moreover, heavy metals, like Pt, can have some problems with fabrication compatibility of standard IC technology.

Manuscript received October 1, 2008. This research was supported by the Dutch Technology Foundation STW (project DET.7213), Applied Science Foundation of NWO, and the technology program of the Ministry of Economic Affairs.

All authors are with the Delft University of Technology, Faculty of Electrical Engineering, Mathematics and Computer Science, Department of Microelectronics, Laboratory for Electronic Components, Technology and Materials (ECTM) and all authors are with the Delft Institute of Microsystems and Nanoelectronics (DIMES) (corresponding author: M. Mihailović, phone: +31-15-2781237; fax: +31-15-2622163; e-mail: m.mihailovic@tudelft.nl).

Last year at SAFE, we presented the concept of the monocrystalline silicon based microhotplate heater [8]. Our heater uses monocrystalline silicon layer for the heating resistor [9]. Monocrystalline silicon is capable for operation up to and above 800 °C [6,10]. The wiring material is titanium silicide. This material is stable at high temperatures and is fabricated in a process that contains relatively little compatibility problems.

The purpose of this paper is to further analyze electrical behaviour of the fabricated mono-Si microheaters and see how it matches theoretical predictions. Also, comparison between two different microheater structures is done to see how different material properties reflect the heater behaviour.

II. Mono-Si microheater

A. Thermal dependence of silicon resistivity

The resistivity of silicon is very much temperature dependent [11] and after successful temperature calibration we would be able to know the temperature by only measuring the electrical resistance of the heater.

The conductivity of silicon is given by $\sigma = q \cdot (\mu_e n + \mu_h p)$, where q is the elementary charge and μ_e, μ_h, n, p - mobility of electrons and holes, and concentration of free electrons and holes, respectively. Total concentration of free electrons equals to $n = N_D + n_i$, where N_D is the concentration of activated donor ions, and n_i - intrinsic electron concentration. Because of the electrical neutrality, the concentration of positively charged carriers can be denoted as $p = n_i^2 / (N_D + n_i)$. At room temperature, the concentration of the charge carriers is initially set by the doping concentration. Therefore n_i can be neglected in respect to N_D, and p in respect to n. With increasing the temperature from room temperature, the resistivity of the silicon ($\rho = \sigma^{-1}$) will also rise. This is due to temperature dependence of the mobility of the charge carriers. However, with further increase of the temperature, more and more charge carriers are thermally generated, thereby contributing to the increase of the conductivity of the material. At a certain temperature (intrinsic temperature), the thermally generated carriers (n_i) will outnumber the activated dopants (N_D) and dominate the conductivity. Under those conditions the material is in the so-called intrinsic region (dopants no more play any significant role). With a further increase of temperature, the resistivity of silicon will drop with the temperature, reaching the values significantly below the

nominal value at room temperature [6, 11, 12].

The described process depends on the concentration of dopants in silicon. As the silicon is more doped, the higher is the intrinsic temperature. Additionally, the ratio of the peak of the resistance (at the intrinsic temperature) and the resistance at room temperature is lower for more doped layers (up to concentrations in order of 10^{18} cm^{-3}) [13].

B. *Design*

Similarly to the most common microheater solutions, our heater has two-dimensional hotplate geometry. It is free standing (thermally insulated) sheet of monocrystalline silicon with the dimensions 500 µm x 300 µm. As shown in Figure 1, the contacts have been made spring-like in order to absorb thermal expansion of the structure. This provides that heater remains in-plane during operation. There are electrical contacts to the device for delivering the power and for measuring the voltage drop. Therefore it contains four contacts in total, making device capable for accurate four-point measurements of the resistance of our heater only, without the effect of the contact resistances introduced by the titanium silicide lines.

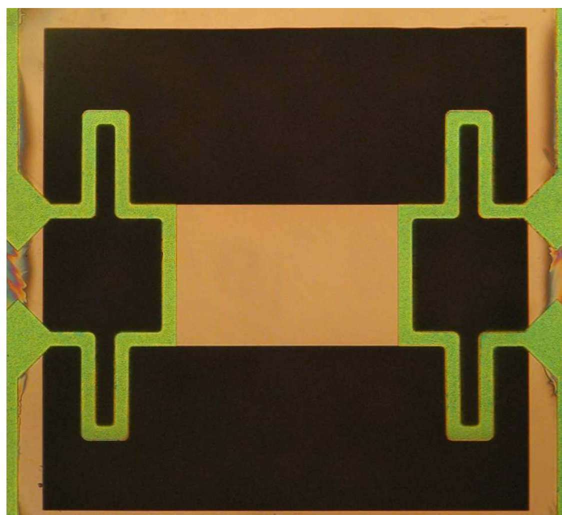

Fig. 1. Optical image of the top view of the device. The black part of the image is completely etched though wafer and the structure is free-standing. The central part is silicon heater of rectangular shape and the green parts form titanium silicide contact wires.

The current is forced through two contacts on different sides of the heater. The voltage across the heater is measured between two remaining contacts: $V_H = V^+ - V^-$. The ratio of the measured voltage and the current $I_H = I_{in} = I_{out}$ (see Fig. 2.a), gives the desired electrical resistance of the heater only ($R_H = V_H / I_H$). The value of R_H changes with the temperature in the similar manner as the resistivity of silicon.

The equivalent electric circuit is shown in Figure 2.b. Four contacts are represented as resistors of the resistance R_{Ci}, where i = 1,2,3,4. (R_{C1} is the resistance of the contact through which the current is fed, and the indices increase in the clockwise direction according to the Figure 2.a.) The heater is modelled as the resistor of the resistance R_H. The power comes out of the ideal current source, and the potential difference across the heater is measured by the voltmeter.

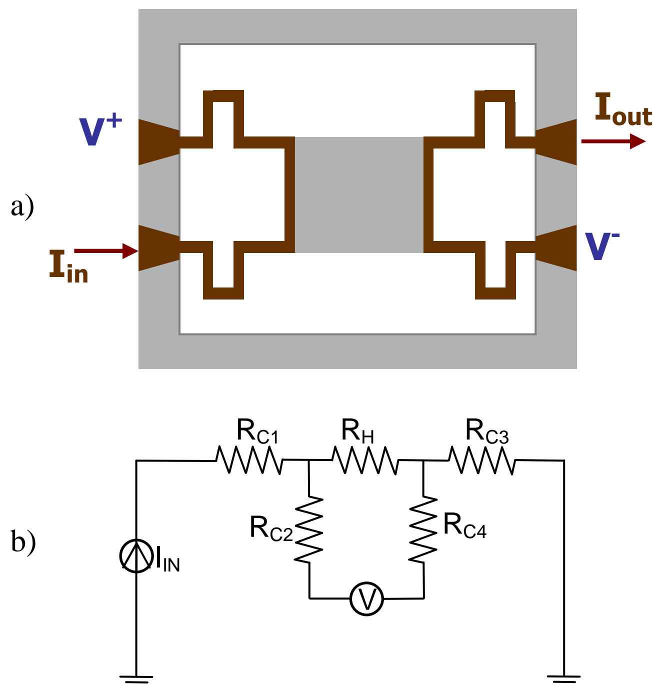

Fig. 2. a) Description of the contacts' role during measurements: the current is fed through two contacts on the opposite sides of the heater, whereas other two contacts sense the voltage across the heater. b) Equivalent electric circuit.

C. *Fabrication*

The devices are fabricated by starting from 100-mm SOI (silicon-on-insulator) wafers. A three masks process is used that could be CMOS compatible with slight modifications.

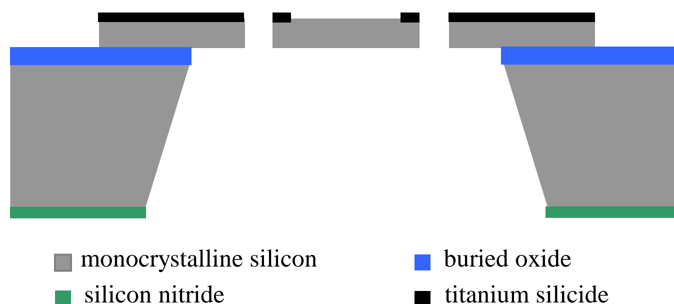

Fig. 3. Schematic cross-section of the device.

The desired silicon resistive layer is obtained through epitaxial growth. There are two sets of the devices that have very similar footprint, but with the different thickness of the epitaxial mono-Si layer. The first set, type A, has the 1 µm thick epi-layer that is doped with As^+ to $5{\cdot}10^{18}$ cm^{-3}, and the second set, type B, has the thicker layer: 5 µm, with the As^+ concentration of $9.5{\cdot}10^{16}$ cm^{-3}. These numbers provide that the sheet resistance values of the silicon layers are in the same level of magnitude.

After silicon nitride deposition and patterning on the back side, 200 nm of titanium is sputtered for the contacts and patterned. The silicon is patterned on the front side, where it is

etched down to the buried oxide. Then, a high temperature annealing at 800 °C is performed, allowing the sputtered titanium to react with the silicon below and form titanium silicide. Then the heaters are released by bulk etching in KOH. The buried oxide at the membranes is stripped in BHF (buffered hydrofluoric acid), to completely release the structure, as illustrated in Figure 3.

III. Measurements

All the electrical measurements were performed using an Agilent 4156C precision semiconductor parameter analyzer and a Cascade probe station.

Firstly, we used test structures on the chip to check the properties of the used layers. These measurement yielded sheet resistance values of $R_{\square TiSi}$ = 1 Ω/□ for titanium silicide and $R_{\square Si}$ = 110 Ω/□ for monocrystalline silicon with the type A. For the type B, results were: $R_{\square TiSi}$ = 0.7 Ω/□ and $R_{\square TiSi}$ = 150 Ω/□.

The principal measurement for device characterization was performed by forcing the current I_H from zero value to 35 mA and measuring V_H as the response. Power dissipated across the heater was calculated as $P_H = I_H \cdot V_H$, and the resistance of the heater as $R_H = V_H / I_H$. The relative change of resistance R_H / R_{H0} (P_H) curve of the type A device is shown in Figure 4. R_{H0} is the heater resistance at room temperature.

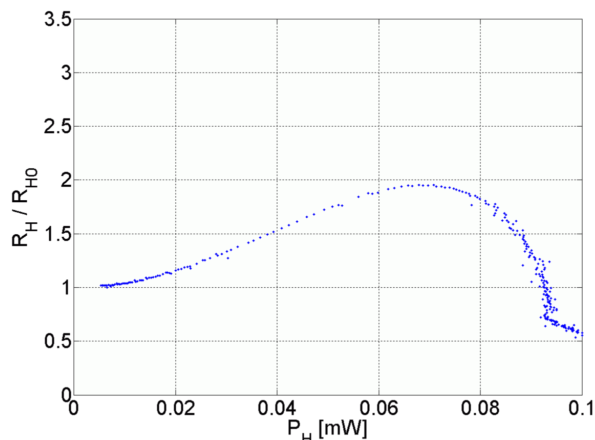

Fig. 4. Relative change of resistance of the heater in dependence of the power dissipated across the heater (type A, Si layer 1 µm thick).

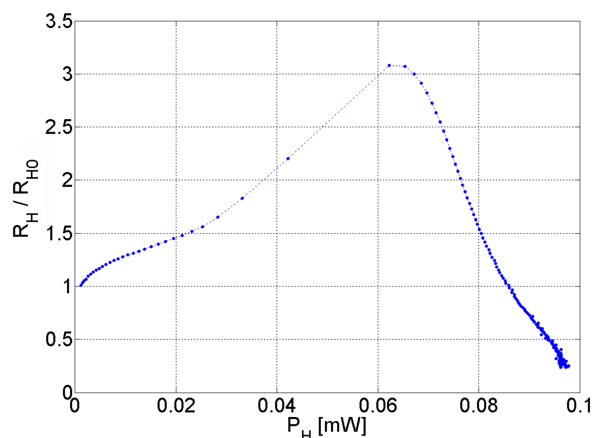

Fig. 5. Relative change of resistance of the heater in dependence of the power dissipated across the heater (type B, Si layer 5 µm thick).

When sufficient power was provided, the heater started glowing in the visible spectrum (first red, then orange).

The same measurement was performed on the devices of the type B. The measured curve is shown in the Figure 5. In this case, visible glowing of the heater body was not observed.

To check the reliability of the proposed method for resistance measurements, a constant power was applied to the device (93.6 mW) for a period of 15 minutes. Time change of the resistance is given in Figure 6.

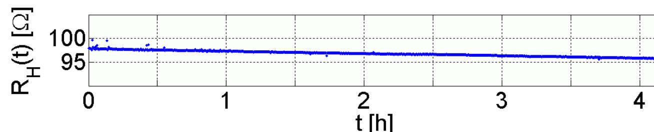

Fig. 6. Time change of the resistance with the constant power supplied (type B, Si layer 5 µm thick).

IV. Discussion

Our fabricated heaters exhibit the expected manner of change of the electrical resistance with temperature. The shape of the curves shown in Figures 4. and 5. is according to the description given in section II.A of this paper.

A. *Heater type A*

Heater of the type A exhibited the increase of the electrical resistance in the order of 2 before reaching the intrinsic temperature (from 180 Ω to 350 Ω). That was followed with the drop below 100 Ω when more power was supplied. The power on the x-axis (see Fig. 4) is only the power dissipated across the heater. This power is related to the temperature of the heater, whereas the total power supplied to the system is higher and is dissipated along the contact wires above the bulk and suspended beams. The input power is in the range of hundreds of milliwatts. For the highest current during the measurement (35 mA), measured voltage was 12.3 V, resulting in 430 mW dissipated in the entire system, with 106 mW dissipated at the heater only.

The exact temperature dependence of the resistance is still not known. After the temperature calibration by putting the device in the furnace and measuring the resistance at known temperatures, it will be possible to determine the temperature of the heater by only measuring resistance.

However, at this moment, based on the electrical measurement and visual inspection, we can claim that the heater has reached temperatures above 600 °C.

As can be seen in the Figure 4, heater passes intrinsic temperature and reaches the intrinsic region during operation. Intrinsic temperature of silicon layers depends on the doping level. As presented in [13], for the silicon layers with the same doping as of type A, intrinsic temperature is in the range above 600 °C.

Another indication of reached high temperatures is the glowing of the heater in the visible spectrum (Figure 7). Thin films start to emit visible thermal radiation above 600 °C [14].

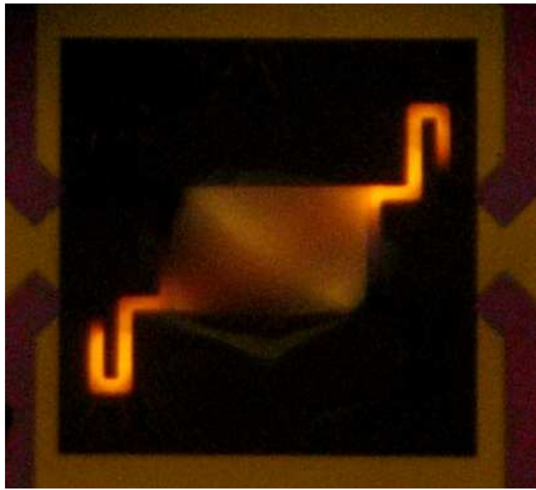

Fig. 7. Optical image of the device in operation (type A, Si layer 1 μm thick). The heater is glowing as well as the contacts for power supply. This is due to the resistance drop of the silicon at high temperatures, which makes the contact resistance important.

Although titanium silicide is very conductive material at room temperature, its resistivity has a constant rise with increasing the temperature, which results in titanium silicide becoming more resistive than silicon at very high temperatures. That is the cause of the lower efficiency of the device at higher temperatures. After the heater starts glowing, heather and contacts are exchanging the roles, with contact wires becoming more resistive and appearing shinier than the heater.

B. Heater type B

The devices of the type B have thicker mono-Si active layer. The consequence is that the volume, and therefore the mass, of the heater body is increased fivefold in respect to the type A. That requires more power in order to reach high temperatures. However, titanium silicide contact wires are being heated more quickly. That limits the dissipation across the heater, even when the total input power is increased. Glowing of the heater body was not observed for the type B, while the silicide in the suspending beams was very hot and intensively glowing yellow and even white.

Despite the noted problems, we can clearly see that the heater was brought to the temperatures of the intrinsic region. For reaching the intrinsic temperature, slightly less power was needed as compared with the device of the type A. But, this time the heater volume is 5 times larger. That means that with the same dissipation across the heater, significantly lower temperatures will be reached. Therefore, we can conclude that intrinsic temperature is for sure lower than in the case of the type A. Further, the ratio of the peak of the resistance and the resistance at room temperature is 3 (increase from 350 Ω to 1.05 kΩ), which is higher than with the type A. That is also according to the expectation.

C. Time stability of the heater under the constant load

Proposed method for temperature measurements based on the resistance measurements can give reliable results when the time response is considered. As shown in Figure 6, time change of the heater resistance, in the course of 4 hours, had the decrease of the resistance with the slope of -0.499 Ω/h from the starting value of 97.84 Ω. The standard deviation from the linear fit is only 0.11 Ω.

V. CONCLUSIONS

In this paper we presented electrical behaviour of microhotplate heater based on monocrystalline silicon. The response of the fabricated devices was tested and devices with two different active layers were compared. Measured results qualitatively confirmed the theoretical expectations. Temperatures achieved with one type of the devices exceed 600 °C.

ACKNOWLEDGEMENT

The authors would like to thank the staff of the ICP group of DIMES Technology Center at Delft University of Technology for their support.

REFERENCES

[1] J. Spannhake, O. Schulz, A. Helwig, G. Müller, and T. Doll, “Design, development and operational concept of an advanced MEMS IR source for miniaturized gas sensor systems”, Proc. 4th IEEE Sensors Conf., Irvine, pp. 762-765, (2005)

[2] D. Briand, A. Krauss, B. van der Schoot, U. Weimar *et al.* “Design and fabrication of high-temperature micro-hotplates for drop-coated gas sensors”, Sensors and Actuators B, vol. 68, pp. 223-233, (2000)

[3] M. Graf, D. Barretino, M. Zimmermann, A. Hierlemann, H. Baltes *et al.* “CMOS monolithic metal-oxide sensor system comprising a microhotplate and associated circuitry”, IEEE Sensors J., vol 4, no. 1, pp. 9-16, (2004)

[4] C. Zhang, K. Najafi, L. P. Bernal, P. D. Washabaugh, “An integrated combustor-thermoelectric micro power generator”, Dig. Transducers ’01, Munich, pp. 34-37, (2001)

[5] N. Kerness, “CMOS-based calorimetric chemical microsensors”, Diss. ETH Zurich, (2002)

[6] L. Sainiemi, K. Grigoras, J. Fan, V. Saarela *et al.* “High-temperature silicon microbridge actuator”, Proc. XXII Eurosensors Conf. Dresden, pp. 806-809, (2008)

[7] S. L. Firebaugh, K. F. Jensen, and M. A. Schmidt, “Investigation of High-Temperature Degradation of Platinum Thin Films with an *In Situ* Resistance Measurement Apparatus”, Journal of Microelectro-mechanical Systems, Vol. 7, No. 1, pp. 128-135, (1998)

[8] M. Mihailović, J.F. Creemer, P.M. Sarro, “Monocrystalline Si-based microhotplate heater”, in Proc. SAFE/STW, Veldhoven, pp. 608-611, (2007)

[9] M.Mihailović, J.F. Creemer, P.M. Sarro, “Monocrystalline silicon microhotplate heater”, Proc. XXII Eurosensors Conf. Dresden, pp. 1611-1614, (2008)

[10] J. Lee, W. P. King, “Microcantilever hotplates: Design, fabrication, and characterization”, Sensors and Actuators A 136 (2007) 291–298

[11] M. Grundmann; The Physics of Semiconductors. Springer, (2006)

[12] W. Fulkerson, J. P. Moore, R. K. Williams, R. S. Graves, and D. L. McElroy, “Thermal Conductivity, Electrical Resistivity, and Seebeck Coefficient of Silicon from 100 to 1300°K”, Physical Review, 167, pp. 765-782, (1967)

[13] J.Kim, S.G. Kim, J.G. Koo, T.M. Roh *et al*. “Characteristics of dynamic resistance in a heavily doped silicon semiconductor resistor”, Int. J. Electronics, vol. 86, pp. 269-279, (1999)

[14] R. M. Tiggelaar, J. W. Berenschot, J. H. de Boer, R. G. P. Sanders, *et al*, “Fabrication and characterization of high-temperature microreactors with thin film heater and sensor patterns in silicon nitride tubes”, Lab on a Chip - Miniaturisation for Chemistry and Biology, 3, p.326 (2005)